The International Journal of Advanced Manufacturing Technology
https://doi.org/10.1007/s00170-023-12290-4

ORIGINAL ARTICLE

A vision-based hole quality assessment technique for robotic drilling of composite materials using a hybrid classification model

Stephen K. H. Lee[1,2,3] · Alexej Simeth[4] · Eoin P. Hinchy[1,2,3] · Peter Plapper[4] · Noel P. O'Dowd[1,2,3] · Conor T. McCarthy[1,2,3]

Received: 4 May 2023 / Accepted: 1 September 2023

Abstract
Robotic drilling has advantages over traditional computer numerical control machines due to its flexibility and dexterity and the potential for rapid production and process automation. The dexterity and reach of the robotic drill end-effector enable the efficient drilling of large composite components, such as aircraft wing structures. Due to the anisotropy and inhomogeneity of fibre-reinforced polymer composite materials, drilling remains a challenging task. Inspection of the drilled hole is required at the end of the process to ensure that the final product is free from defects. Typically, such inspections require the parts to be transferred to a dedicated inspection station, which is a time-consuming non-value-added task and impractical for large components. In the interest of an efficient and sustainable manufacturing process, this work proposes a hybrid classification model implemented with a robotic drilling system to investigate the quality of drilled holes in situ. The classifier is trained and tested with a random selection of drilled holes, and the most accurate classifier is implemented. The selected classifier returns 90% overall prediction accuracy on unseen drilled holes. This machine learning–based approach, using a convolutional neural network and support vector machine classifier, can significantly improve inspection reliability while reducing production time for drilled composite components. This is the first study that demonstrates a hole quality assessment technique for robotic drilling of composite material in situ at scale.

Keywords Machine learning · Convolutional neural network · Support vector machine · Composite material · Drilling · Industrial robotics

1 Introduction

Carbon fibre–reinforced polymer (CFRP) composite structures are widely used in the aerospace industry where their high strength-to-weight ratio is crucial to reducing operational costs [1]. Machining processes such as drilling are often required to join different aerospace components, such as skin-stringer fuselage joints [2]. Traditionally, drilling of composite structures is conducted using computer numerical control (CNC) machine centres or articulating industrial robotic drills. The frames of CNC machine centres have very high mechanical stiffness, and as such, they are renowned for producing holes with high accuracy and precision. However, CNC machining often requires parts to be loaded into the machine manually which is a non-value-added step. Robotic drilling allows in situ processing, which in return can increase throughput; however, industrial articulating robots traditionally have lower stiffness characteristics and positional accuracy compared to CNC machine centres. To date, the advancement of robotic arms for machining applications has demonstrated significant performance improvements over the earlier generations [3, 4]. Bu et al. [5] studied the relationship between robot stiffness and hole quality, where it was reported that a higher robot stiffness, achieved by optimising the drilling posture, resulted in improved drilling

✉ Stephen K. H. Lee
stephen.lee@ul.ie

Eoin P. Hinchy
Eoin.Hinchy@ul.ie

1 Confirm Smart Manufacturing Research Centre, Limerick, Ireland

2 School of Engineering, University of Limerick, Limerick V94 T9PX, Ireland

3 Bernal Institute, University of Limerick, Limerick V94 T9PX, Ireland

4 Faculty of Science, Technology and Medicine, University of Luxembourg, Esch-Sur-Alzette, Luxembourg

Published online: 27 September 2023

stability and accuracy. In addition, the robotic drilling data collected can be used to develop smart manufacturing applications such as digital twin technology, which can further increase efficiency by facilitating real-time monitoring and decision-making [6, 7].

Limiting damage during the drilling of composite structures is an important consideration which needs to be addressed when designing the drilling process [8, 9]. Almost 60% of part rejections during the final assembly of aerospace components are due to excessive damage introduced by drilling [10]. Therefore, it is crucial to ensure that drilling processes are well executed and ideally have the ability to adapt in real time to minimise damage. Damage introduced during the drilling of composite materials includes delamination, uncut fibres, rough surfaces and other hole defects [11, 12]. Such defects can impact the reliability and longevity of riveted and bolted structural joints. Improper selection of drilling process parameters can also increase the severity of the defects. A high drilling thrust force, which is generally associated with a high feed rate, can lead to delamination, one of the most severe damage mechanisms in composite drilling [13–16]. While it is generally accepted that thrust force is not strongly influenced by spindle speed [17], tool wear is strongly dependent on spindle speed which has an effect on hole damage [16].

To address these concerns, an inspection procedure is typically performed after a hole is drilled. Non-destructive testing techniques including C-scan, X-ray, digital photography and thermography are commonly used for inspecting aerospace structures [10, 14, 18–26]. The advantage of C-scan and X-ray techniques is their ability to allow the detection and characterisation of interlaminar delamination damage [27, 28]. These techniques however are highly specialised, and we found that it is impractical to perform rapidly in a production line, hence requiring the laminates to be transferred for inspection which results in a delay. Similarly, Teti et al. [29] reported that most inspection methods are limited to laboratory techniques largely due to the practical limitations caused by access problems during machining, poor lighting conditions and usage of coolant. Therefore, digital photography is a suitable alternative as it can be easily implemented in an industrial environment for a fast and cost-effective inspection [24]. Although digital photography only inspects surface damage, it provides a practical and rapid solution to identify damaged holes directly on the production line. Hole inspection in CFRP laminates using digital photography can be challenging. To achieve a clear visual of the damage, Cui et al. [25] developed a vision inspection station to perform a comprehensive method to segment the damage of a drilled hole. Hrechuk et al. [22] used the Moore-Neighbor tracing algorithm and the Delaunay triangulation method to define a damage contour with optical microscopy. Maghami et al. [26] designed and developed a multi-light imaging robotic end-effector to achieve a clear visual of the component by ensuring even lighting is omitted at the drilled hole for inspection. These investigations were carried out in a controlled environment and were performed manually at the end of the drilling process. Process downtime inevitably increases as a result of time spent setting up the inspection station and/or delays associated with the preparation of the workpiece for inspection. To achieve an efficient and sustainable production process, it is essential therefore that the process downtime and inspection time are kept at a minimum. Therefore, the method proposed in this paper does not use a bespoke system but aims to inspect the hole quality in situ using the machine vision system already available in the drilling end-effector. Studies on robotic in situ inspection technique have been reported in the literature over recent years. Yu et al. [30] developed an in-process countersink inspection method for aluminium approach based on machine vision in automated drilling and riveting system. Li et al. [31] developed a deep learning approach for circular hole detection on composite part for a robotic drilling system. However, their work did not investigate the hole quality, which is a step forward from hole detection. Hence, the advantage of the approach developed in this work over [30] and [31] is the ability to predict the quality of a drilled hole on composite material.

Recent research has examined the use of deep neural networks for feature recognition, quality prediction, process monitoring and optimisation of manufacturing processes [32, 33]. Through machine learning and deep learning, complex features can be identified automatically from training data. Such approaches are relatively insensitive to variations and are versatile in detecting distinct features in various application conditions [34]. These include using a convolutional neural network (CNN) to automate the vision-based inspection of CFRP composites [26], a tele-operated robot to detect defects on an aircraft surface using a deep learning algorithm [35] and visual inspection combined with deep learning to quantify the condition of the fastening bolts of a train [36]. CNNs are designed to work with image data, and a support vector machine (SVM) is a robust generic classifier developed to classify multiple-dimensional space data. Combining a CNN with an SVM can achieve strong feature representation from an image and a strong classifier. Another benefit of using a CNN is that it preserves the spatial information of an image, which enhances prediction accuracy [37]. In this work, the CNN is used to extract image features to train a SVM classifier to classify new images. It follows from work in [38], where a combined CNN-SVM was used to detect fluid level in bores for an assembly process. To this end, a hybrid classification model consisting of a pretrained CNN and a SVM classifier is developed. The proposed model is implemented in a robotic drilling system to quantify the quality of drilled holes in CFRP in situ, with the

aim to increase inspection efficiency and reduce downtime associated with the post-process inspection steps.

This work aims to assess the accuracy and reliability of the proposed classification model applied to a robotic drilling system. The objectives of this work are (i) identification of a suitable classifier for classifying drilled holes in CFRP, (ii) investigation of the performance of SVM classifiers trained with features extracted by a pre-trained CNN from a dataset of drilled holes and (iii) investigation of the practicability of the system for in situ monitoring of robotic drilling of composite materials in an industrial environment. The remaining structure of the paper is as follows: Section 2 of this paper describes the methodology of the approach; Section 3.1 explains how the data are prepared and showcases how the model performs; Section 3.2 contains the results and discussion, and finally, Section 4 provides concluding remarks on this work and suggests potential future work.

2 Methodology

In this work, a CNN is combined with a SVM image classifier to provide a hybrid classification model to classify the quality of drilled holes in CFRP panels. The hybrid classification model is applied to an industrial robot with a vision-system-equipped end-effector for in situ inspection. The classification task is reduced to a binary problem with images of drilled holes classified into either "class 1" or "class 2," representing different amounts of damage, to be discussed in Section 2.1.

A schematic of the training methodology for the hybrid model is shown in Fig. 1, where the workflow is illustrated. The workflow is split into the data preparation phase (Fig. 1a) and the modelling stage (Fig. 1b). After a hole is drilled, an image of the hole is captured, pre-processed and categorised. Data are then augmented to increase the dataset size (the augmentation process is discussed in Section 2.4). Next, the augmented dataset is split into training and test datasets in the ratio of 70:30, with an equal number of class 1 and class 2 holes in each dataset. Note that we exclude the original hole images from the augmented dataset used for training and testing. These images are used in the final validation step (see Fig. 1b). If one class is under-represented in the augmented dataset, a balanced dataset is achieved by randomly selecting the same number of data in the under-sampled class from the oversampled class. A pre-trained CNN architecture (ResNet50, a CNN with 50 layers) is then used to extract a number of image features from each image in the training dataset to train the SVM classifier. The trained SVM classifier is then used to classify the holes in the test dataset, and the prediction accuracy for the test dataset is determined. This procedure is repeated 500 times with a different 70:30 random selection of training and test data. A SVM classifier identifies a hyperplane (decision boundaries) in an N-dimensional space (depending on the number of features) that classifies the data points [39]. Every trained SVM classifier will thus have a unique hyperplane, depending on the training data used. The prediction accuracy of the classifier is determined by the sum of images classified correctly divided by the total number of images used for classification. The classifier which returns the highest prediction accuracy

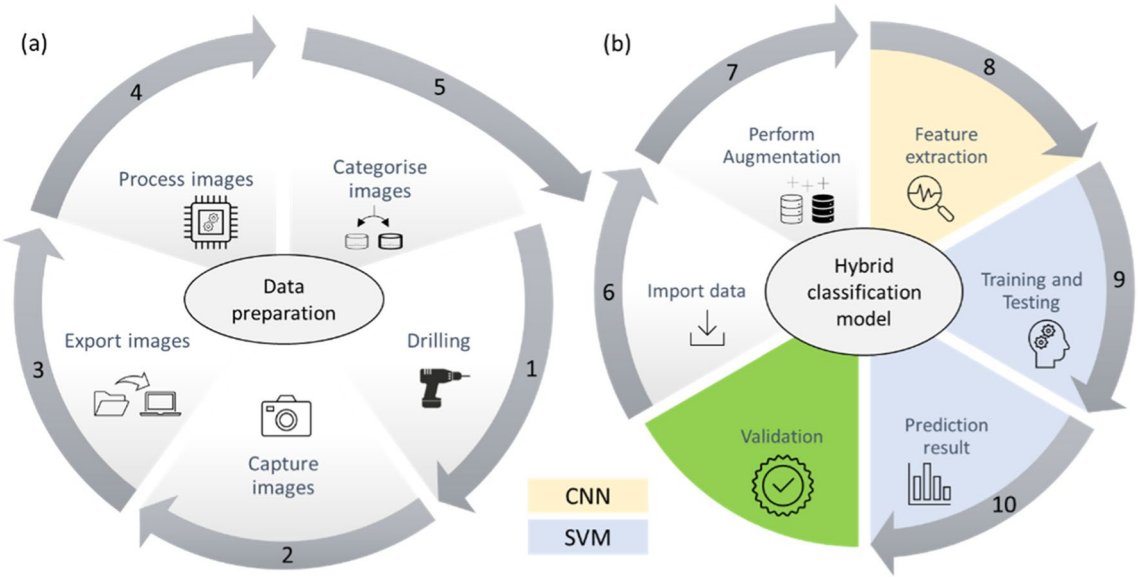

Fig. 1 **a** Process flow of data collection and processing; **b** process flow for SVM and CNN

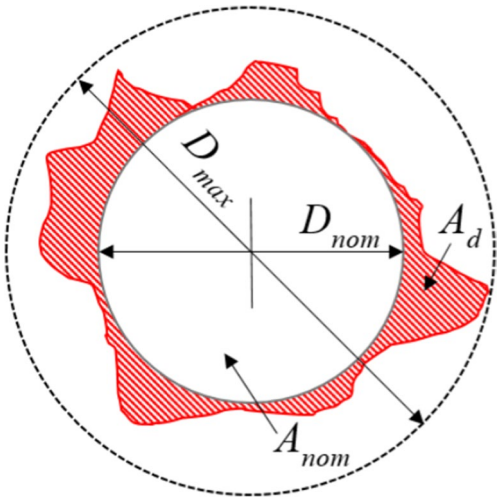

Fig. 2 Schematic illustrating key features of delamination (adapted from Davim et al. [23])

from the test dataset is selected. A validation step is then carried out using the original image dataset, which was not included in the training and testing dataset.

2.1 Delamination analysis

Damage due to delamination is quantified using a delamination factor. Figure 2 illustrates the key features of drilling-induced damage for a hole. The hatched red region in the figure denotes the delamination area, D_{nom} is the nominal hole diameter, and D_{max} is the maximum diameter of the delamination zone. Several methods for quantifying delamination have been proposed. Chen [40] proposed a delamination factor, F_d as

$$F_d = \frac{D_{\text{max}}}{D_{\text{nom}}} \tag{1}$$

To account for irregular surface damage induced by the drilling of composite materials, Davim et al. [23] proposed an adjusted delamination factor (F_{da}), where

$$F_{da} = F_d\left(1 + \frac{A_d}{A_{max} - A_{nom}}\left(F_d - 1\right)\right) \tag{2}$$

As seen in Fig. 2, A_d is the area of the damaged zone. A_{nom} in Eq. 2 is the nominal hole area and A_{max} is the circular area corresponding to D_{max}. From Eqs. 1 and 2, $F_{\text{da}} = F_d = 1$ corresponds to an undamaged hole. Evaluation of F_{da} thus requires identification of D_{max} and A_d for each hole.

In this work, the delamination factor, F_{da}, is used to categorise the drilled hole into two classes: a class 1 defect is defined as $1.0 \le F_{\text{da}} \le 1.65$ and class 2 defect as $F_{\text{da}} > 1.65$. Therefore, in this case, class 1 is an acceptable hole, and class 2 is an unacceptable hole. The classification threshold of 1.65 was determined based on visual assessment. A clear discrimination has been observed at that value of F_{da}, with holes for which $F_{\text{da}} > 1.65$ have a significantly greater level of damage. However, while the threshold is specified in the current paper, this value can be modified for a given application. For example, in an application which may have a more strict damage tolerance, the threshold value of F_{da} to define a class 1 or 2 hole could be lowered to 1.4 or below. The objective of this study is to demonstrate that the classification model can be trained and implemented in a robotic drilling setup for in situ inspection and is independent of the threshold value chosen.

2.2 Experimental setup

2.2.1 Materials

Carbon fibre composite laminates were manufactured from aerospace grade HexPly® 8552/IM7 high-performance carbon fibre impregnated with epoxy. The composite has a 1.77 g/cm^3 fibre density (57.7% nominal fibre volume) [41]. Two laminate stacking sequences were used, both consisting of 32 prepreg plies, $[0]_{16\ s}$ and $[0, +45, 90, -45]_{4\ s}$. The laminates were cured in an LBBC Technologies TC 1000 THPT autoclave at 180 °C for 6 h. The final thickness of the laminates was measured at 4 mm using a Mitutoyo Vernier calliper. Panels of size 150 mm × 150 mm were extracted from the laminate via waterjet cutting using a Maxiem 1530 abrasive waterjet. A diamond-like coating (DLC) carbide drill bit was used to drill the holes, see Table 1. The hole spacing is 20 mm, and a total of 25 holes are drilled in each panel.

2.2.2 Robotic drilling and vision system

Drilling was performed by a KUKA KR210 six-axis industrial robotic arm equipped with a multifunctional end-effector, see Fig. 3. The robot arm has a reach of 2.7 m and a maximum payload of 210 kg. The end-effector consists of a drilling module and a vision module, both operating on the same axis. Dry drilling conditions are used with vacuum extraction, and the workpiece is mounted onto the support structure using a bolted joint. The drilling process parameters are provided in Table 2.

Table 1 Technical specifications of the drill bit

Material	DLC carbide tool
Diameter	4.8 mm
Geometry	Twist drill
Point angle	135°
Helix angle	30°

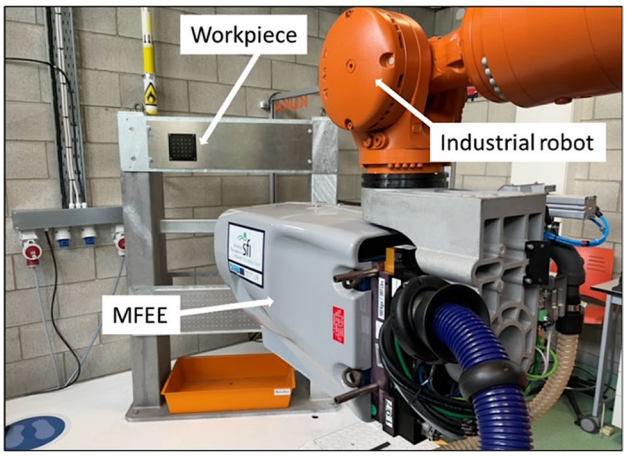

Fig. 3 Photograph showing industrial robot, multifunctional end-effector and composite workpiece

Table 2 Drilling process parameters used for machining the carbon fibre composite material

Feed speed	0.01–0.2 mm/rev
Rotation speed	1500–10,000 rpm
Clamping force	400 N

The vision system consists of a vision module and a Cognex In-Sight 5400 series industrial camera with a resolution of 640 × 480 pixels. The vision module is composed of an angle converter and ring lighting. The camera captures an image of the drilled hole once drilling is complete, as illustrated in Fig. 4. Bitmap images are exported from the camera to a local PC via Profinet/IO network protocol and are then extracted to a remote laptop via ethernet connection for further processing.

2.3 Data preparation

A standard laptop is used to process the digital image. A MATLAB script imports, rotates, flips and crops the images to a resolution of 140 × 264 pixels, as shown in Fig. 5. Images are analysed manually using ImageJ version 1.53 k [42], and the delamination factor, F_{da}, is determined after creating a binary mask of the damaged area. Images are then categorised into class 1 or class 2, see Fig. 6, based on the value of F_{da} as discussed in Section 2.1.

2.4 Image augmentation

Image augmentation is a technique used to artificially expand a dataset [43]. It is helpful when a dataset is small and can be more cost-effective than further data collection. In this study, 308 images of drilled holes were collected. The augmenter rotates images by random angles, resizes the images by a random scale factor, shears images horizontally (XShear) and vertically (YShear) by a random angle and translates images horizontally (XTranslation) and vertically (YTranslation) by a random distance. The respective parameters (ranges) for the different augmentation functions are outlined in Table 3.

3 Hybrid classification model

3.1 Training procedure

Figure 7 provides more details of the training procedure presented in Fig. 1b. First, the data are pre-processed and sorted into classes. Each class is then augmented using the augmentation procedure described in Section 2.4. A total of 308 original images (118 in class 1 and 190 in class 2) are increased to 2006 class 1 and

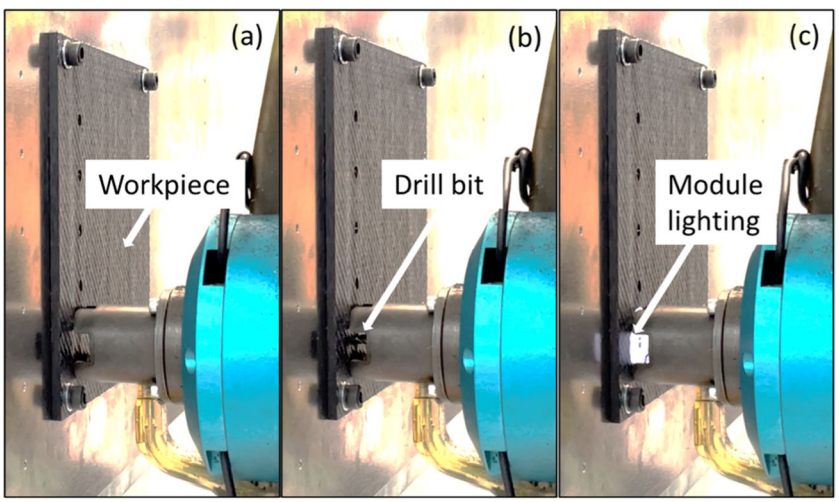

Fig. 4 Photographs of robotic drilling process. **a** Robot clamps onto the workpiece, **b** drilling operation, **c** in situ inspection

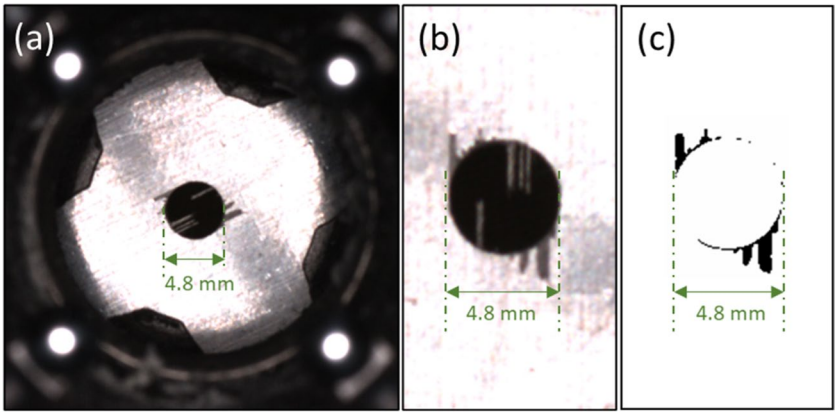

Fig. 5 Image processing operations to determine the damaged area: **a** raw image; **b** processed image; **c** binary mask of the damaged area

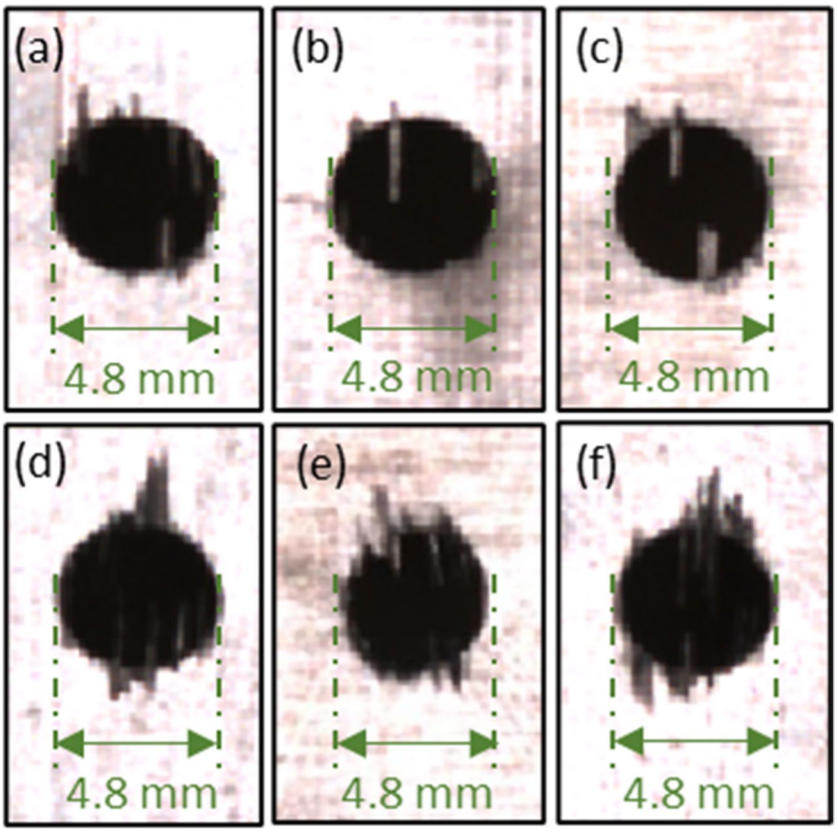

Fig. 6 Photographs showing examples of class 1 (**a**–**c**) and class 2 (**d**–**f**) defect holes

Table 3 Augmentation functions and parameters used for images in this study

Function	Parameters
Rotation	[0, 30°]
Scale	[0.8, 1.2]
XShear	[0.8, 1.2°]
YShear	[0.8, 1.2°]
XTranslation	[0, 10 pixels]
YTranslation	[0, 10 pixels]

2090 class 2 images, respectively. To achieve a balanced dataset for both classes, 2006 images are randomly selected from the 2090 class 2 images. Next, the dataset is randomly divided using a 70:30 split for training data (1404 images) and test data (601) for each class. Then, 1000 features are extracted for each image by the CNN to train the SVM classifier. Finally, the trained classifier is tested on the test dataset from both classes. The time to classify each image is recorded. To assess the performance of the SVM classifier, the classes predicted by the classifier are compared to the actual classes. This process is repeated 500 times for both training and test datasets.

After 500 iterations, the SVM classifier with the highest prediction accuracy is applied to the original 308

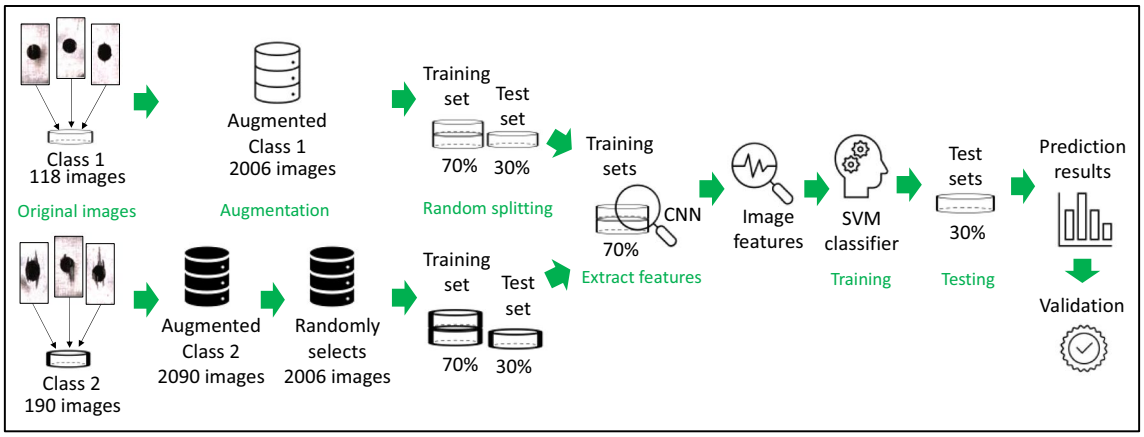

Fig. 7 Schematic showing the process flow for training the classification model

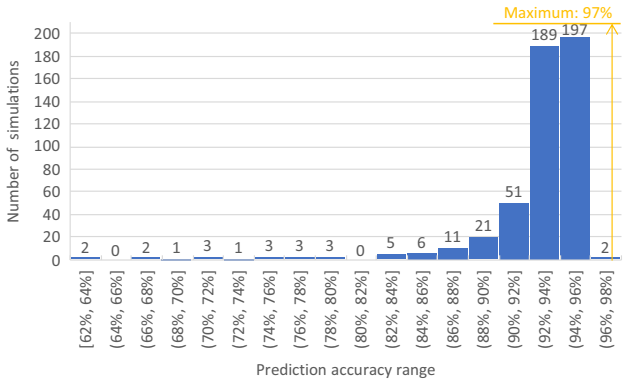

Fig. 8 Graph plotting the number of simulations vs. prediction accuracy range of 500 training and testing cycles using the augmented dataset

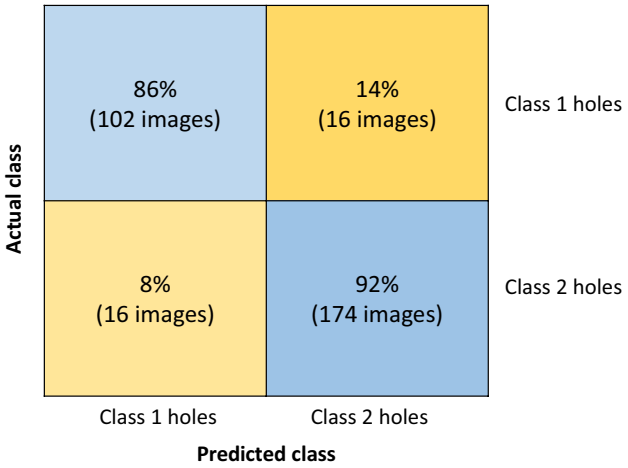

Fig. 9 Prediction accuracy of first classifier in the 96–98% band applied to the original dataset

images as a validation step. The hybrid classification model is implemented in MATLAB 2021a and runs on a desktop with Windows 10 Pro, an Intel Xeon W-2135 processor, and 32 GB RAM. The average prediction time per hole is 0.16 s for this dataset, which includes the time to read the image and classify the hole.

3.2 Results and discussion

The accuracy of the SVM classifier in the prediction of 500 training and testing cycles on the augmented dataset ranges from 62 to 97%, as shown in Fig. 8. The classifier that returns the highest accuracy is selected. In this case, two classifiers fall within the 96–98% accuracy band on test data. The predictions of the first classifier on the original dataset are shown in Fig. 9. This classifier correctly predicts 86% of class 1 images and 92% of class 2 images in the original dataset. Fourteen percent of the class 1 images have been misclassified to class 2, and 8% of class 2 images

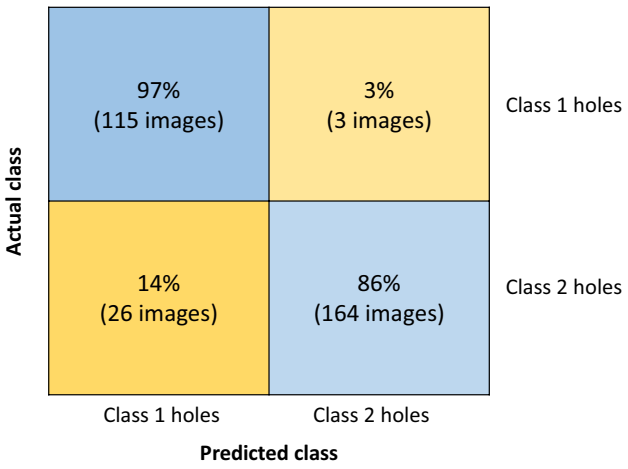

Fig. 10 Prediction accuracy of second classifier in the 96–98% band applied to the original dataset

have been misclassified to class 1. Thus, this classifier has higher performance on low-quality (class 2) holes at 92%. The predictions of the second classifier are shown in Fig. 10. This classifier misclassified 14% of class 2 images as class 1. It is considered that the consequence of misclassification is more severe when a class 2 (low quality) hole is classified as a class 1 (high quality) hole. This scenario may lead to sub-standard, defective holes being approved for use in manufacturing, with potentially detrimental effects. Thus, the importance of correctly classifying class 2 holes is a key consideration for this work, and therefore, the first classifier has been selected. This classifier has an overall prediction accuracy of 97% on the test dataset and 90% on the original image dataset.

The results of these preliminary investigations can be improved by (i) training a CNN model specifically for quantifying drilled CFRP panels, (ii) using transfer learning which decreases the training time, and (iii) using alternative data augmentation methods, such as synthetic minority oversampling technique (SMOTE) which takes similar images and merges them into one, based on the *k*-nearest neighbours algorithm [44]. The augmentation procedure in Table 3 performed well on the original dataset, despite the fact that the use of translation and shear functions is not realistic in the setup depicted in Fig. 4, where the drill bit and camera are along the same axis. Omitting translate and shear during augmentation may improve the classifier performance.

Challenges in hole quality evaluation of drilled holes in CFRP panels have recently been examined, including developing new methodologies [22, 24] and the use of multi-light imaging [26]. While these studies showed good results in principle, these reported techniques may not be feasible for in situ inspection. In [30], an in-process inspection method to measure the countersink dimensions in countersunk holes in aluminium is presented. A hybrid inspection method was developed to process the images captured in an automated drilling and riveting system. The proposed inspection approach achieved a normal deviation angle and countersink depth at less than 0.15° and within 0.02 mm, respectively. Although this approach is accurate, it may not be suitable for CFRP application due to its distinct mechanical properties and special anisotropic and non-homogenous features [45]. A composite surface poses a challenge for visual measurement, in particular during segmenting the damage and the circular hole detection process. To overcome this, a semi-supervised deep learning method to segment and detect circular holes on a composite part was developed in [31]. An extensive image processing routine was performed to generate enough training data for the model. Once trained, their model achieved a 95% accuracy in determining the circumference of circular drilled holes. The studies in [30] and [31] focused on the preliminary steps (detection) of a hole inspection process and are not easily generalised to determine hole quality, which is the interest of this paper. Investigation of hole quality on composite material using a robotic drill in situ was not addressed. An extensive literature search has found no prior investigation on such a study, incorporating both hole monitoring and determination of hole quality. To the authors' knowledge, the work presented in this manuscript using a CNN-SVM model is the first study that demonstrates an accurate prediction of hole quality in situ using a robotic drilling setup, representative of a manufacturing environment.

It is important to highlight that this model is trained based on the features extracted from a set of images taken by a low-resolution camera with a pre-trained CNN. This approach avoids the requirement of a computationally intensive image processing step in conjunction with high-resolution imaging to evaluate the damage profile of a drilled hole, as adopted in [22, 26]. The benefits of the method proposed in this work are the reduced effort for manual calibration and image processing and the suitability of the method for in situ applications (production line or factory scale level) where machining and inspection can be performed in real time. This approach can have a significant impact on, for example, aircraft manufacture, which typically involves millions of drilled holes during assembly. It may also be noted that the compute time for the training of this hybrid classifier (which uses a pre-trained CNN for image feature extraction) is significantly less than training a CNN from scratch, which would require thousands of images.

4 Conclusion

This study demonstrates an automated in situ inspection methodology for a robotic drilling process. The proposed in situ inspection with a trained hybrid classification model can be used to minimise downtime of a production line by integrating the inspection step into a robotic drilling process.

An industrial robot, equipped with an end-effector, is used to perform both drilling and inspection. A hybrid classification model, consisting of a pre-trained convolutional neural network (CNN) and a support vector machine (SVM) image classifier, has been developed to categorise images of drilled holes in carbon fibre–reinforced polymer panels into two classes. Random features extracted from the images by the CNN were used to train the SVM classifier. Five hundred simulations of random training and test data were cross-validated to address the variability of the trained classifier. The classifier was selected based on the percentage of misclassification between classes. The prediction accuracy of the selected classifier on unseen data is 90%. The trained classifier was implemented in the robotic drilling process and can

classify drilled hole images into class 1 and class 2 based on the image features without the need for further image post-processing. While the model showed high prediction accuracy at 90%, it should be noted that there are limitations with this technique, where only surface damage is detectable. Possible areas for future work include (i) training a model to predict hole damage on the far side based on the hole surface damage and drilling process parameters to achieve a robust all-rounded in situ vision-based inspection technique and (ii) process optimisation of robotic drilling based on the hole quality prediction results.

Acknowledgements The publication has emanated from research conducted in the Confirm Smart Manufacturing Research Centre, with the financial support of Science Foundation Ireland (SFI) under Grant Number SFI/16/RC/3918, co-funded by the European Regional Development Fund. The author would like to thank Mr. Tayfun Durmaz, Dr. Ahmad Farhadi, and Dr. Karthik Ramaswamy for their guidance and support for this work.

Author contributions Stephen K. H. Lee: investigation, writing-original draft, methodology, data curation, and validation. Alexej Simeth: software, data curation, investigation, validation, and writing—review and editing. Eoin P. Hinchy: writing (review and editing) and supervision. Peter Plapper: supervision. Noel P. O'Dowd: writing (review and editing) and supervision. Conor T. McCarthy: writing (review and editing), supervision, and funding acquisition.

Declarations

Ethical approval Not applicable.

Consent to participate Not applicable.

Consent for publication The authors agree to publish this work.

Conflict of interest The authors declare no competing interests.

References

1. Krishnaraj V, Prabukarthi A, Ramanathan A et al (2012) Optimization of machining parameters at high speed drilling of carbon fiber reinforced plastic (CFRP) laminates. Compos B Eng 43:1791–1799. https://doi.org/10.1016/j.compositesb.2012.01.007
2. Grutta JT, Miskioglu I, Charoenphan S, Vable M (2000) Strength of bolted joints in composites under concentrated moment. J Compos Mater 34:1242–1262. https://doi.org/10.1106/L5A3-WFQ3-N7B0-EQET
3. Bi S, Liang J (2011) Robotic drilling system for titanium structures. Int J Adv Manuf Technol 54:767–774. https://doi.org/10.1007/s00170-010-2962-2
4. Pereira B, Griffiths CA, Birch B, Rees A (2021) Optimization of an autonomous robotic drilling system for the machining of aluminum aerospace alloys. Int J Adv Manuf Technol. https://doi.org/10.1007/s00170-021-08483-4
5. Bu Y, Liao W, Tian W et al (2017) Stiffness analysis and optimization in robotic drilling application. Precis Eng 49:388–400. https://doi.org/10.1016/j.precisioneng.2017.04.001
6. Farhadi A, Lee SKH, Hinchy EP et al (2022) The development of a digital twin framework for an industrial robotic drilling process. Sensors 22:7232. https://doi.org/10.3390/s22197232
7. Barbosa GF, Shiki SB, Savazzi JO (2019) Digitalization of a standard robot arm toward 4th industrial revolution. Int J Adv Manuf Technol 105:2707–2720. https://doi.org/10.1007/s00170-019-04523-2
8. Xu J, Geier N, Shen J et al (2023) A review on CFRP drilling: fundamental mechanisms, damage issues, and approaches toward high-quality drilling. J Market Res 24:9677–9707. https://doi.org/10.1016/j.jmrt.2023.05.023
9. Geng D, Liu Y, Shao Z et al (2019) Delamination formation, evaluation and suppression during drilling of composite laminates: a review. Compos Struct 216:168–186. https://doi.org/10.1016/j.compstruct.2019.02.099
10. Khashaba UA (2004) Delamination in drilling GFR-thermoset composites. Compos Struct 63:313–327. https://doi.org/10.1016/S0263-8223(03)00180-6
11. Slamani M, Gauthier S, Chatelain J-F (2016) Comparison of surface roughness quality obtained by high speed CNC trimming and high speed robotic trimming for CFRP laminate. Robot Comput-Integr Manuf 42:63–72. https://doi.org/10.1016/j.rcim.2016.05.004
12. Davim JP, Reis P (2003) Drilling carbon fiber reinforced plastics manufactured by autoclave—experimental and statistical study. Mater Des 24:315–324. https://doi.org/10.1016/S0261-3069(03)00062-1
13. Hocheng H, Tsao CC (2006) Effects of special drill bits on drilling-induced delamination of composite materials. Int J Mach Tools Manuf 46:1403–1416. https://doi.org/10.1016/j.ijmachtools.2005.10.004
14. Hocheng H, Tsao CC (2003) Comprehensive analysis of delamination in drilling of composite materials with various drill bits. J Mater Process Technol 140:335–339. https://doi.org/10.1016/S0924-0136(03)00749-0
15. Tsao CC, Hocheng H (2007) Effect of tool wear on delamination in drilling composite materials. Int J Mech Sci 49:983–988. https://doi.org/10.1016/j.ijmecsci.2007.01.001
16. Lin SC, Chen IK (1996) Drilling carbon fiber-reinforced composite material at high speed. Wear 194:156–162. https://doi.org/10.1016/0043-1648(95)06831-7
17. Geier N, Szalay T (2017) Optimisation of process parameters for the orbital and conventional drilling of uni-directional carbon fibre-reinforced polymers (UD-CFRP). Measurement 110:319–334. https://doi.org/10.1016/j.measurement.2017.07.007
18. Tsao CC, Hocheng H (2005) Computerized tomography and C-scan for measuring delamination in the drilling of composite materials using various drills. Int J Mach Tools Manuf 45:1282–1287. https://doi.org/10.1016/j.ijmachtools.2005.01.009
19. Dilonardo E, Nacucchi M, De Pascalis F et al (2020) High resolution X-ray computed tomography: a versatile non-destructive tool to characterize CFRP-based aircraft composite elements. Compos Sci Technol 192:108093. https://doi.org/10.1016/j.compscitech.2020.108093
20. Saoudi J, Zitoune R, Gururaja S et al (2016) Prediction of critical thrust force for exit-ply delamination during drilling composite laminates: thermo-mechanical analysis. Int J Mach Mach Mater 18:77. https://doi.org/10.1504/IJMMM.2016.075464
21. Babu J, Paul Alex N, Abraham SP et al (2018) Development of a comprehensive delamination assessment factor and its evaluation with high-speed drilling of composite laminates using a twist drill. Proc Inst Mech Eng B: J Eng Manuf 232:2109–2121. https://doi.org/10.1177/0954405417690552
22. Hrechuk A, Bushlya V, Ståhl J-E (2018) Hole-quality evaluation in drilling fiber-reinforced composites. Compos Struct 204:378–387. https://doi.org/10.1016/j.compstruct.2018.07.105

23. Davim JP, Rubio JC, Abrao AM (2007) A novel approach based on digital image analysis to evaluate the delamination factor after drilling composite laminates. Compos Sci Technol 67:1939–1945. https://doi.org/10.1016/j.compscitech.2006.10.009
24. Cui J, Liu W, Zhang Y et al (2021) A novel method for predicting delamination of carbon fiber reinforced plastic (CFRP) based on multi-sensor data. Mech Syst Signal Process 157:107708. https://doi.org/10.1016/j.ymssp.2021.107708
25. Cui J, Liu W, Zhang Y et al (2022) A visual inspection method for delamination extraction and quantification of carbon fiber reinforced plastic (CFRP). Measurement 111252. https://doi.org/10.1016/j.measurement.2022.111252
26. Maghami A, Salehi M, Khoshdarregi M (2021) Automated vision-based inspection of drilled CFRP composites using multi-light imaging and deep learning. CIRP J Manuf Sci Technol 35:441–453. https://doi.org/10.1016/j.cirpj.2021.07.015
27. Xu J, Li C, Mi S et al (2018) Study of drilling-induced defects for CFRP composites using new criteria. Compos Struct 201:1076–1087. https://doi.org/10.1016/j.compstruct.2018.06.051
28. Haeger A, Schoen G, Lissek F et al (2016) Non-destructive detection of drilling-induced delamination in CFRP and its effect on mechanical properties. Procedia Eng 149:130–142. https://doi.org/10.1016/j.proeng.2016.06.647
29. Teti R, Jemielniak K, O'Donnell G, Dornfeld D (2010) Advanced monitoring of machining operations. CIRP Ann 59:717–739. https://doi.org/10.1016/j.cirp.2010.05.010
30. Yu L, Bi Q, Ji Y et al (2019) Vision based in-process inspection for countersink in automated drilling and riveting. Precis Eng 58:35–46. https://doi.org/10.1016/j.precisioneng.2019.05.002
31. Li G, Yang S, Cao S et al (2021) A semi-supervised deep learning approach for circular hole detection on composite parts. Vis Comput 37. https://doi.org/10.1007/s00371-020-01812-w
32. Mongan PG, Hinchy EP, O'Dowd NP, McCarthy CT (2021) Quality prediction of ultrasonically welded joints using a hybrid machine learning model. J Manuf Process 71:571–579. https://doi.org/10.1016/j.jmapro.2021.09.044
33. Mongan PG, Modi V, McLaughlin JW et al (2022) Multi-objective optimisation of ultrasonically welded dissimilar joints through machine learning. J Intell Manuf 33:1125–1138. https://doi.org/10.1007/s10845-022-01911-6
34. Zheng X, Zheng S, Kong Y, Chen J (2021) Recent advances in surface defect inspection of industrial products using deep learning techniques. Int J Adv Manuf Technol 113:35–58. https://doi.org/10.1007/s00170-021-06592-8
35. Ramalingam B, Manuel V-H, Elara MR et al (2019) Visual inspection of the aircraft surface using a teleoperated reconfigurable climbing robot and enhanced deep learning technique. Int J Aerospace Eng 2019:1–14. https://doi.org/10.1155/2019/5137139
36. Zhou F, Song Y, Liu L, Zheng D (2018) Automated visual inspection of target parts for train safety based on deep learning. IET Int Transport Syst 12:550–555. https://doi.org/10.1049/iet-its.2016.0338
37. Syberfeldt A, Vuoluterä F (2020) Image processing based on deep neural networks for detecting quality problems in paper bag production. Procedia CIRP 93:1224–1229. https://doi.org/10.1016/j.procir.2020.04.158
38. Simeth A, Plaßmann J, Plapper P (2021) Detection of fluid level in bores for batch size one assembly automation using convolutional neural network. In: Dolgui A, Bernard A, Lemoine D et al (eds) Advances in production management systems. Artificial Intelligence for Sustainable and Resilient Production Systems. Springer International Publishing, Cham, pp 86–93
39. Gandhi R (2018) Support vector machine — introduction to machine learning algorithms. In: towardsdatascience. https://towardsdatascience.com/support-vector-machine-introduction-to-machine-learning-algorithms-934a444fca47. Accessed 16 Feb 2023
40. Chen W-C (1997) Some experimental investigations in the drilling of carbon fiber-reinforced plastic (CFRP) composite laminates. Int J Mach Tools Manuf 37:1097–1108. https://doi.org/10.1016/S0890-6955(96)00095-8
41. Hexcel (2020) HexPly® 8552 EU technical data Sheet. https://energy.ornl.gov/CFCrush/materials/uou/8552_eu.pdf
42. Schneider CA, Rasband WS, Eliceiri KW (2012) NIH image to ImageJ: 25 years of image analysis. Nat Methods 9:671–675. https://doi.org/10.1038/nmeth.2089
43. Allred R (2018) Image augmentation for deep learning using Keras and histogram equalization. In: Medium. https://towardsdatascience.com/image-augmentation-for-deep-learning-using-keras-and-histogram-equalization-9329f6ae5085. Accessed 27 Sep 2022
44. Bhattacharya A (2022) How to use SMOTE for dealing with imbalanced image dataset for solving classification problems. In: The Startup. https://medium.com/swlh/how-to-use-smote-for-dealing-with-imbalanced-image-dataset-for-solving-classification-problems-3aba7d2b9cad. Accessed 10 Feb 2023
45. Zhang Y, Wu D, Chen K (2019) A theoretical model for predicting the CFRP drilling-countersinking thrust force of stacks. Compos Struct 209:337–348. https://doi.org/10.1016/j.compstruct.2018.10.107